Prediction of the earthquake magnitude by time series methods along the East Anatolian Fault, Turkey

Article *in* Earth Science Informatics · September 2021

DOI: 10.1007/s12145-021-00636-z

3 authors:

Hatice Çekim
Hacettepe University
26 PUBLICATIONS **258** CITATIONS
SEE PROFILE

Senem Tekin
Adıyaman University
121 PUBLICATIONS **621** CITATIONS
SEE PROFILE

Gamze Özel Kadilar
Hacettepe University
176 PUBLICATIONS **1,901** CITATIONS
SEE PROFILE

Earth Science Informatics
https://doi.org/10.1007/s12145-021-00636-z

RESEARCH ARTICLE

Prediction of the earthquake magnitude by time series methods along the East Anatolian Fault, Turkey

Hatice Oncel Cekim[1] · **Senem Tekin**[2] · **Gamze Özel**[1]

Received: 13 March 2021 / Accepted: 19 May 2021

Abstract
In this study, the magnitude of an earthquake in the East Anatolian Fault (EAF) of Turkey are predicted based on previous earthquakes whose magnitudes are four or more by two-time series methods, namely autoregressive integrated moving average (ARIMA) and singular spectrum analysis (SSA). These methods are quite new in seismology despite being successful techniques in other branches of science. We use ARIMA and SSA models to train and predict the mean and maximum values of the earthquakes' magnitudes due to seismological events between years 1900 and 2019. 447 earthquake magnitudes between 1900 and 1995 are used for training models, and then 447 magnitudes between 1995 and 2019 are taken into account for testing. The root mean square error (RMSE) is calculated to evaluate the accuracy of each model. The results demonstrate that the SSA model is better than the ARIMA model to predict the earthquake magnitude. Hence, for the years 2020 to 2030 the magnitude of an earthquake is forecasted using the SSA model. The result shows that the highest magnitude of earthquake is forecasted for the year 2021 in magnitude level of 4.0–5.9.

Keywords Earthquake prediction · Time series analysis · ARIMA · Singular spectrum analysis

Introduction

Earthquakes have been one of the most hazardous but least predictable natural disasters. The occurrence of catastrophic earthquakes results in casualties, massive damage to the infrastructure, the vanquishing of societies in a flash and a sudden downfall in the country's economy. Turkey ranks high among countries that have suffered centuries of loss of life and property due to earthquakes since the country is one of the world's most active seismic zones located on the Alpine-Himalayan seismic belt. 43% of the country's surface area is located in areas with an expected acceleration value greater than 0.40 g, defined as the first degree earthquake zone. In the past years, the earthquake that occurred in Turkey has caused great damage leading to loss of life and property. Therefore, several local and regional seismic hazard studies (Aslan 1972; Bath 1979; Yarar et al. 1980; Erdik et al. 1999; Kayabalı and Akın 2003; Bayrak et al. 2005, 2009; Akkar et al. 2018) have been performed in order to estimate the seismic hazard in Turkey using the statistical processing of instrumental earthquake data.

Turkey's most critical tectonic characteristics are the Aegean Arc, the West Anatolian Graben Complexes, the North Anatolian Fault (NAF), the East Anatolian Fault (EAF), the North East Anatolian Fault and the Bitlis Thrust Zone. The EAF constitutes an essential part of Turkey's tectonic structure, Anatolia 4–13 mm on the due westward movement of the plates/year being left-lateral characters (Hempton 1985; Arpat and Saroglu 1972; Dewey et al. 1986; Allen et al. 2004; Westaway 1994; Aksoy et al. 2007; Duman and Emre 2013; Bulut 2017).

The EAF has caused many devastating earthquakes of 6 or more magnitudes in the historical and instrumental period. It is known that the segments that make up the EAF have the potential to produce earthquakes with an

Communicated by: H. Babaie.

✉ Hatice Oncel Cekim
oncelhatice@hacettepe.edu.tr

Senem Tekin
senemtekin@adiyaman.edu.tr

Gamze Özel
gamzeozl@hacettepe.edu.tr

[1] Department of Statistics, Hacettepe University, Beytepe 06800 Ankara, Turkey

[2] Department of Mining and Mineral Extraction, Adıyaman University, 02040 Adiyaman, Turkey

Published online: 15 June 2021

instrumental size of 6 or more on the segments according to their lengths. Considering the instrumental magnitude, it is seen that the middle and NE (northern east) parts of the EAF are seismically active in the instrumental period. The instrumental magnitude of the most massive earthquake that occurred on the segments in the last century is Ms = 6.9 (On January 24, 2020, at 8:55 pm Turkey local time, the Elazığ-Sivrice earthquake, which was the epicenter of Sivrice with a north latitude of 39.10 east longitudes of 38.35 and a magnitude (Mw) of 6.8 occurred. The quake was felt mostly in the nearby cities many provinces such as Elazig and Malatya, Adıyaman, Kahramanmaraş, Adana, Hatay, Osmaniye, Tunceli, Gaziantep, Şanlıurfa cities in the region, as well.). Therefore, the prediction of destructive earthquakes in the EAF zone is an essential tool to extract information for the prevention and risk reduction of casualties after strong earthquakes.

Numerous researchers have performed earthquake studies from the prediction and hazard assessment through different angles. The basic model is the Gutenberg Richter (GR) model that states the frequency's logarithm is linearly dependent on the magnitude. However, Dargahi-Noubary (1986) and Kagan (1993) suggest that more suitable statistical models should be used instead of the GR model for the distribution with high magnitudes. Petersen et al. (2007) proposed a time-independent model showing that the probability of earthquake occurrence follows the Poisson distribution. Considering the time of earthquakes, stochastic processes, especially Poisson processes, have also been used to predict the number of earthquakes. However, the Poisson model cannot be sufficient since it has an exponential recurrence time distribution and a constant hazard function. This assumes that the probability of observing an earthquake at any given time is independent of both elapsed time since the last earthquake and its severity. This assumption leads only to time-independent seismic hazard estimates. Besides, earthquakes are clustered in time and space and their distribution is over-dispersed compared to the Poisson law. Other stochastic processes including compound Poisson processes by Özel and Inal (2008), Özel (2011), branching processes by Kagan (2007), Jackson and Kagan (2006), and point processes by Helmstetter and Sornette (2003), Ogata (2017) have been used for the prediction of the number of earthquakes. On the other hand, the earthquake's size or magnitude could not be predicted easily by the stochastic process. Furthermore, the seasonality and trends of earthquakes cannot be evaluated by those methods.

In recent times, taking into account the seasonality and trends of earthquakes, the prediction of the size or magnitude has been performed in a few studies by time series models such as Auto-Regressive Integrated Moving Average (ARIMA) and generalized autoregressive conditional heteroskedasticity (GARCH) (Shishegaran et al. 2019; Zhu 2012). However, the singular spectrum analysis (SSA) has not been used before to forecast the magnitude of earthquakes in a seismic region. The SSA is a nonparametric novel and powerful time series analysis technique incorporating classical time series analysis, multivariate statistics, multivariate geometry, dynamical systems, and signal processing. This new method can be useful for the prediction of the earthquake magnitude in a seismic region (Serita et al. 2005; Guo et al. 2019). The SSA can extract important seismological time series components with characteristic irregular behavior and provide good forecasts for them. Therefore, this study's main aim is to show the SSA method's performance in seismic studies.

This paper contributes to the literature in two ways. First of all, existing studies generally do not account for time-effects, leading to omitted variable bias. The SSA method has not been used before for the prediction of the magnitude of earthquakes. However, this study captures the dynamics of earthquake occurrence using a novel SSA method to predict earthquake magnitude in the EAF with time-effects, often omitted in estimations. Secondly, both average and maximum earthquake magnitudes have been obtained for the first time ARIMA and SSA models.

The rest of the paper is organized as follows: The study area and data are described in Sect. 2 and then, the methodology is presented in Sect. 3. The models are applied to achieve the earthquake magnitude prediction aim in the EAF line in Sect. 4 and the results are given in Sect. 4. The conclusion is given in Sect. 5.

Material

In this study, the earthquake data of the EAF for the years 1900 and 2019 have been obtained from the Republic of Turkey Prime Ministry, Disaster & Emergency Management Authority, Presidential of Earthquake Department (DEMA 2020). Figure 1 shows the study area taken from the Earthquake Department (DEMA 2020). The EAF, whose general direction is NE-SW, is approximately 580 km long (Emre et al. 2013). As seen in Fig. 1, the left-lateral strike-slip EAF in Turkey, which forms the boundary between the Arabian Plate and the Anatolian block, intersects with the North Anatolian Fault (NAF) in Karlıova in the northeast and the Dead Sea Fault (DSF) around Kahramanmaraş in the southwest. Table 1 shows the fault parameters for active faults in the updated active fault of the EAF. The EAF, which has a left-sided strike-throw feature, consists of six segments: Karlıova, Ilıca, Palu, Pütürge, Erkenek, Pazarcık and Amanos.

According to historical and instrumental earthquake records, it is known that earthquakes of magnitude 6.8 and larger occur in each of the six segments. Considering the lengths of the segments, it can be said that each of

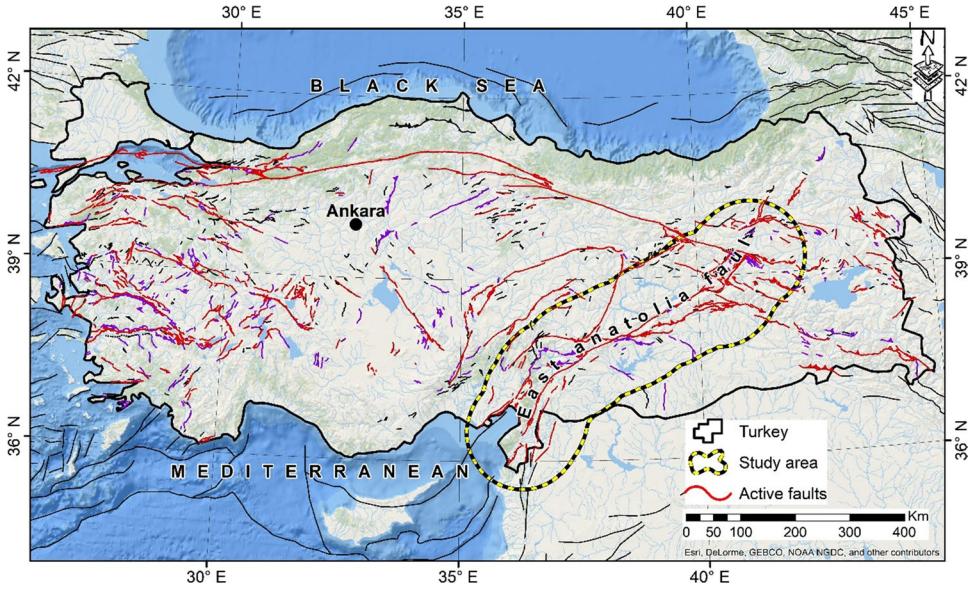

Fig. 1 Active faults of Turkey (Emre et al. 2013) and location map of in this study

them has the potential to produce an earthquake with an instrumental magnitude of 7.0 and more giant (Duman et al. 2018).

Turkey on the segments that make up the EAF based on historical earthquake catalog. There are 146 earthquakes with a magnitude of 5 and above (Fig. 2a). Twenty of these significant earthquakes that caused tremendous damage and caused more than 20 km surface rupture, 1822 Antakya Earthquake, 1866 Göynük-Karlıova, 1872 Lake Amik Earthquake, 1874 and 1875 Tortum-Hazar Lake Earthquakes, 1893 Malatya Earthquake, 1457 Erzincan-Erzurum, 1046 Diyarbakır-Elazığ and 242 Osmaniye earthquakes. According to the instrumental period (1900-present) earthquake records, 917 earthquakes developed four and above (Fig. 2b). The most massive quake with 6.9 magnitudes occurred on August 19, 1966 in the Varto district of Muş located on the EAF. Two thousand three hundred ninety-four people died due to this earthquake. The last earthquake on the EAF was 6.8 magnitude on January 24, 2020. This earthquake was felt in many cities in Turkey, including Elazığ, Malatya, Kahramanmaraş, Adıyaman, especially Batman, Bingöl, Çorum, Diyarbakır, Gaziantep, Hatay, Mardin, Osmaniye, Samsun, Sivas, Siirt, Şanlıurfa, Şırnak, Tokat and Tunceli. While 41 people lost their lives, massive damage occurred in nearly 1000 buildings.

Methodology

Autoregressive integrated moving average (ARIMA) model

ARIMA, also known as Box-Jenkins models, is divided into seasonal and non-seasonal models. Non-seasonal Box-Jenkins models are generally shown as ARIMA (p, d, q), where p is the parameter of the autoregression (AR) model, d is the number of difference procedure, and q is the parameter of the moving average (MA) model. The ARIMA (p, d, q) model equation is in the form of

Table 1 The summary of the fault parameters for active faults in the updated active fault of the EAF (Emre et al. 2013)

		Length (km)	Activity	Slip type	General trend	Dip direction and degree of the fault plane
Fault	EAF	580	H	LLS		
Segment	Karlıova Segment	31	H	LLS	N50E	Vertical
	Ilıca Segment	40	SF	LLS	N40E	Vertical
	Palu Segment	77	H	LLS	N62E	Vertical
	Pütürge Segment	96	H	LLS	N60E	Vertical
	Erkenek Segment	62	H	LLS	N75E	Vertical
	Pazarcık Segment	82	H	LLS	N60E	Vertical
	Amanos Segment	112	H	LLS	N35E	Vertical

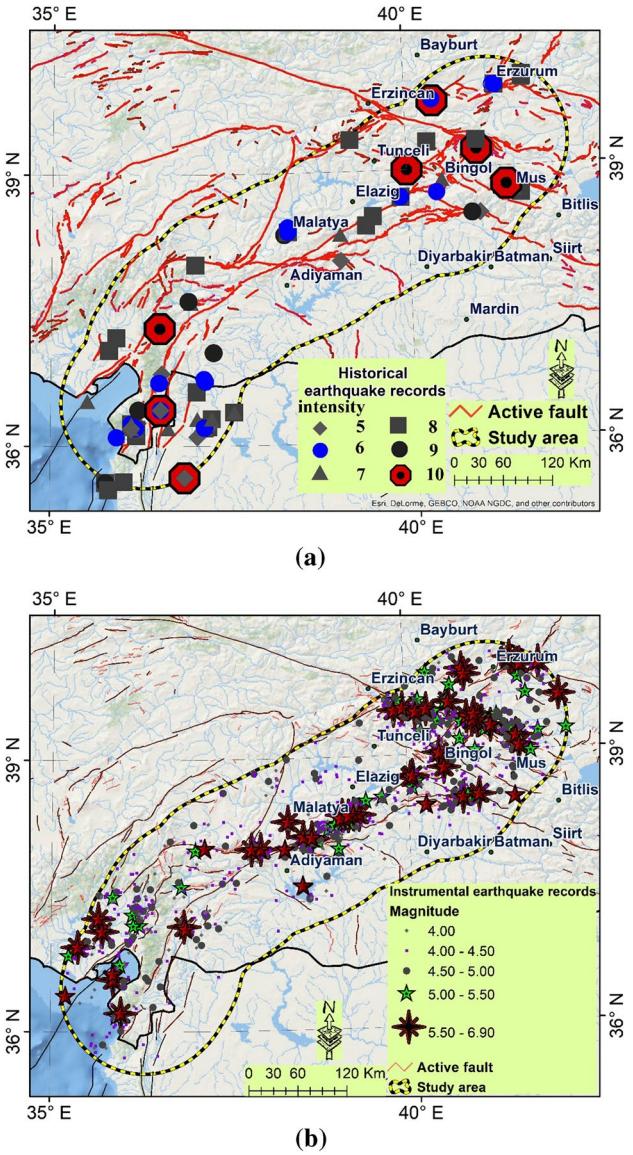

Fig. 2 Historical (Başarır Baştürk et al. 2017) (**a**), Instrumental (Kadirioğlu et al. 2018) (**b**) earthquake records for EAF

$$\phi_p(D)\nabla^d Z_t = \theta_q \omega_t$$

where Z_t is a time series, ω_t is the error series,$\nabla^d = (1-D)^d$ is the difference operator, D is the backshift operator, $\phi_p(D) = (1 - \phi_1 D - \phi_2 D^2 - \cdots - \phi_p D^p)$ is the AR term at the pth order, and $\theta_q(D) = (1 - \theta_1 D - \theta_2 D^2 - \cdots - \phi_q D^q)$ is the MA term at the qth order (Lai and Dzombak 2020).

To perform the analysis processes of the Box-Jenkins method, first, care should be taken to ensure that the series is free of trend and seasonal fluctuations, that is, the series should be stationary. Then, determine the p and q parameters depending on the autocorrelation function and the partial autocorrelation function graphs and control the model parameters' significance. Lastly, the root mean square error criterion (RMSE) is used to selects the best model among the models having the white noise error series (Zang et al. 2020).

SSA (Single Spectrum Analysis) Method

The SSA technique has been used in a variety of fields such as signal processing (Kumaresan and Tufts 1980), nonlinear dynamics (Broomhead and King 1986; Fraedrich 1986), climate (Vautard and Ghil 1989; Ghil and Vautard 1991; Yiou et al. 1996), medicine (Pereira and Maciel 2001) and mathematical statistics (Moskvina and Zhigljavsky 2003). SSA has also been used as an efficient pre-processing algorithm to avoid the effect of discontinuous or intermittent signals, coupled with neural networks (or similar approaches) for time series forecasting (Sivapragasam et al. 2001; Deng 2014).

The SSA is a time series forecasting method that is frequently preferred to analyze the periodic oscillation in the series. It is quite advantageous to work with the SSA method considering that it is a non-parametric analysis and has a superior performance compared to other time series methods. The SSA method decomposes a time series into some components with simpler structures, such as a slowly varying trend, oscillations and noise. The necessary steps of SSA are as follows:

i. The first step is to create the multidimensional matrix X by determining the suitable window length W, $1 < W < N/2$, where N is the time series length. This length W is achieved experimentally. Also, choice of this suitable length is subject to the interested problem and preliminary information of the time series. In the selection of window length, rules valid for all situations cannot be given. However, there is a suggestion that the window length should be selected as the common multiples of 12 (Gao et al. 2020). The created multidimensional matrix X is defined as:

$$X = \begin{bmatrix} X_1 & X_2 & \cdots & X_{N-W+1} \\ X_2 & X_3 & \cdots & X_{N-W+2} \\ \cdots & \cdots & \cdots & \cdots \\ X_W & X_{W+1} & \cdots & X_N \end{bmatrix}$$

ii. Decomposition of the matrix X is performed to obtain $S = XX^T$ by separating the eigenvalue ($\lambda_1 \geq \cdots \geq \lambda_W \geq 0$). $X = X_1 + X_2 + \cdots + X_W$ is obtained from this stage, such that $X_i = \sqrt{\lambda_i} \wedge_i A_i^T$, $A_i = X^T \wedge_i / \sqrt{\lambda_i}$ and $\wedge_1, \wedge_2, \ldots, \wedge_W$ is the j th eigenvector (Golyandina and Zhigljavsky 2013).

iii. The elementary matrices are divided as the basic matrices of $X_i, (1, 2, \ldots, W)$ into several groups and

Table 2 Descriptive statistics of the variables AEM and MEM for the years 1900 to 2019

	Min	Max	Mean	Median	St. Deviation	Skewness	Kurtosis	ADF Test	SW (P-Value)
AEM (Mw)	4	6	4.763	4.655	0.492	0.745	-0.453	0.01	<0.001
MEM (Mw)	4	6.9	5.304	5.200	0.612	0.445	-0.011	0.01	0.019

generated the matrices by summing in each group using the p eigentriples.

iv. The diagonal averaging step, according to the reconstruction of the one-dimensional series, can be subsequently a converted matrix with chosen singular values to derive the Hankel matrix process (Xiao et al. 2019).

The RMSE criterion is a frequently used criterion to compare different methods in time series and various study areas. We calculated the RMSE values to find the best predictions among the used methods in this article (Hassani et al. 2020; Silva et al. 2018). The RMSE formula is expressed as (Naim and Mahara 2018).

$RMSE\sqrt{\frac{1}{N}\sum_{k-1}^{N}(Z_k-\hat{Z}_{k|ki1})^2}$,

where z_k indicates the actual value and $\hat{Z}_{k|ki1}$ represents the k^{th} forecast value considering the previous value of $k=1,2,...,N$.

Results

The earthquake data of the EAF in Turkey between the years 1900 and 2019 have been obtained from the Republic of Turkey Prime Ministry, Disaster & Emergency Management Authority, Presidential of Earthquake Department. The magnitudes are then evaluated by two variables: the average earthquake magnitude (AEM) and the maximum earthquake magnitude (MEM). The data period range is between 1900 and 2019. It is crucial to determine the models' fit by comparing the actual values with the predictions (Hyndman and Athanasopoulos 2018). Therefore, we split the data set into training and test data to empower accuracy and reduce the error rate. 20% of the total data are taken into account as the test data between 1996 and 2019. The years 1900–1995 are considered the training data, consisting of 80% of the total data.

The descriptive statistics in Table 2 provide information about the values of AEM and MEM between the years 1900 and 2019.

As seen in Table 2, the recorded AEM values are ranged from 4 to 6 Mw, whereas the values of the MEM changes between the values 4 Mw and 6.9 Mw. The averages of AEM and MEM are 4.763 Mw and 5.304 Mw, respectively, for the years 1900 to 2019. Besides positive values of the skewness for these series, the right-skewed data and negative kurtosis values of two variables indicate flatted distributions. Moreover, the Shapiro–Wilk (SW) test for the normality shows that these variables data are not normally distributed. In this situation, it is necessary to use non-parametric methods for the prediction of earthquake magnitude.

Figure 3 indicates the time series of two variables in this paper. These series are stationary according to the Augmented Dickey-Fuller (ADF) test given in Table 2.

Figure 3 shows that the EAF, which was active until 1960, shrinks after 1960 with a decreasing trend in earthquake magnitudes in the AEM series. On the other hand, in the MEM series, it was observed that until 1980, the maximum earthquake magnitudes between 4 and 7 Mw magnitudes occurred in sudden ups and downs, and after 1980 these sudden movements decreased.

In this study, time series models ARIMA and SSA have been studied to prediction of both average and maximum earthquake magnitudes. A free licensed version of R statistics software with "Rssa" and "forecast" packages (https://rstudio.com/products/rstudio/download/) is used for the analysis of these methods. Now, the first model ARIMA

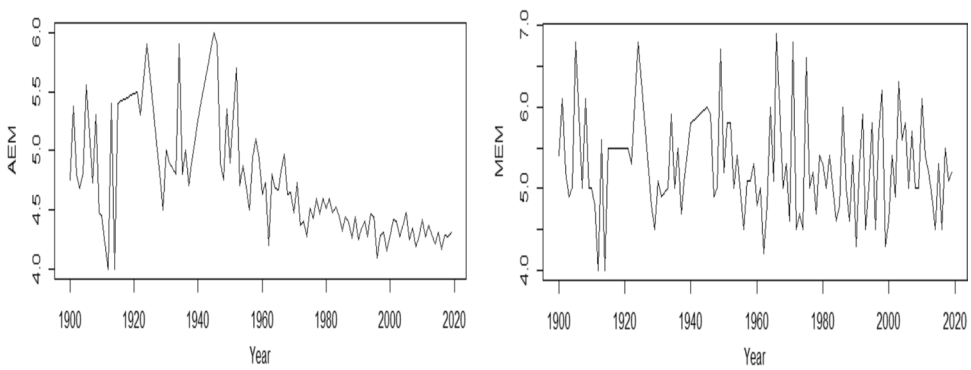

Fig. 3 The plots of time series for the variables AEM and MEM at the EAF in Turkey from the years 1900 to 2019

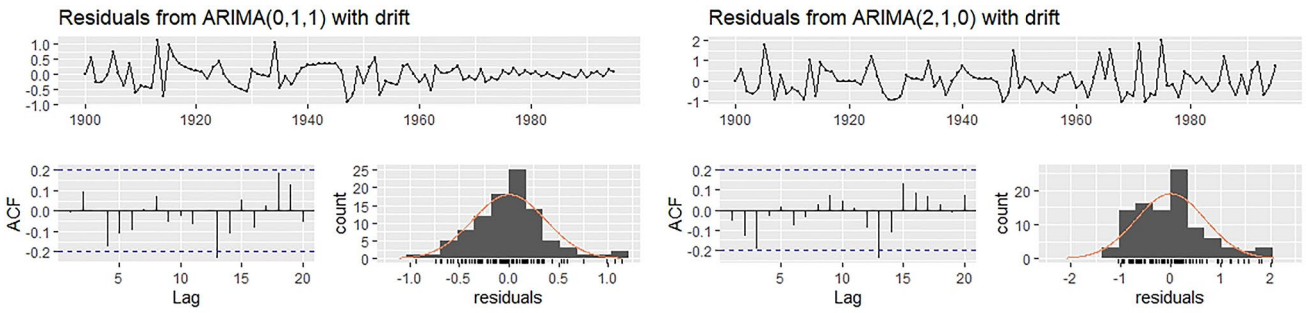

Fig. 4 The white noise control of the error series obtained from the models for the AEM and MEM series

Table 3 The RMSE values obtained according to the optimum models

	Variables	
Methods	AEM	MEM
ARIMA	0.117 ARIMA (0,1,1)	0.570 ARIMA (2,1,0)
SSA	0.108 SSA(12,4)	0.551 SSA(12,10)

has been conducted and hence the considered series must be stationary. Figure 4 represents that the error series of the model is white noise. Then, the ARIMA model with both significant coefficient (P-values < 0.05) and the lowest RMSE value (See Table 3) is selected. After completing all steps of ARIMA, the best models for the AEM and MEM are determined as ARIMA (0,1,1) and ARIMA (2,1,0), respectively.

The second model is the SSA. The decomposition of series is performed firstly with the SSA method. In this process, the window width is designed as a multiple of 12. Window width (W), periodic sorting and decomposition of series are tested for all width sizes. Moreover, with the help of the W-correlation matrix, those with strong associations between the principal components (p) are placed in the same group. The optimum window widths of 12 are determined from Fig. 5 for two variables.

Figure 6 shows the trend, seasonal and error components of the AEM and MEM series, separated step by step with the SSA method. The method takes into account the properties of these components for AEM and MEM predictions. The prediction steps are available for this method, including single and combined. This model first independently forecasts the three components utilizing the decomposition step (as in Fig. 6). Then, all components' predicted values are aggregated into a combined result as a reconstruction step (as in Fig. 7). Figure 7 captures the ups and downs of the original series of trend components. Trend and seasonal components together closely follow the fluctuations of the original series. When we evaluate Figs. 6 and 7 together, it is seen that the trend components of the two series have a flexible structure that takes extreme values. On the other hand, the effect of seasonal components is in the fluctuations of the series. As

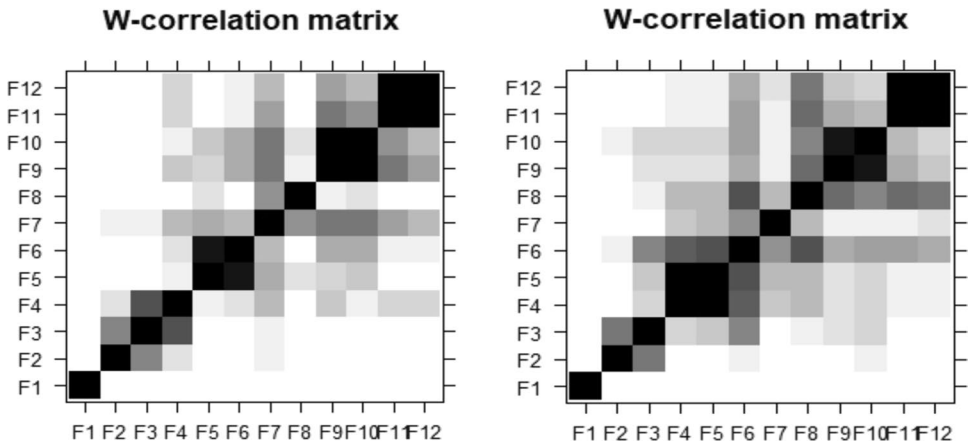

Fig. 5 The W-correlation matrix graphs for AEM and MEM series

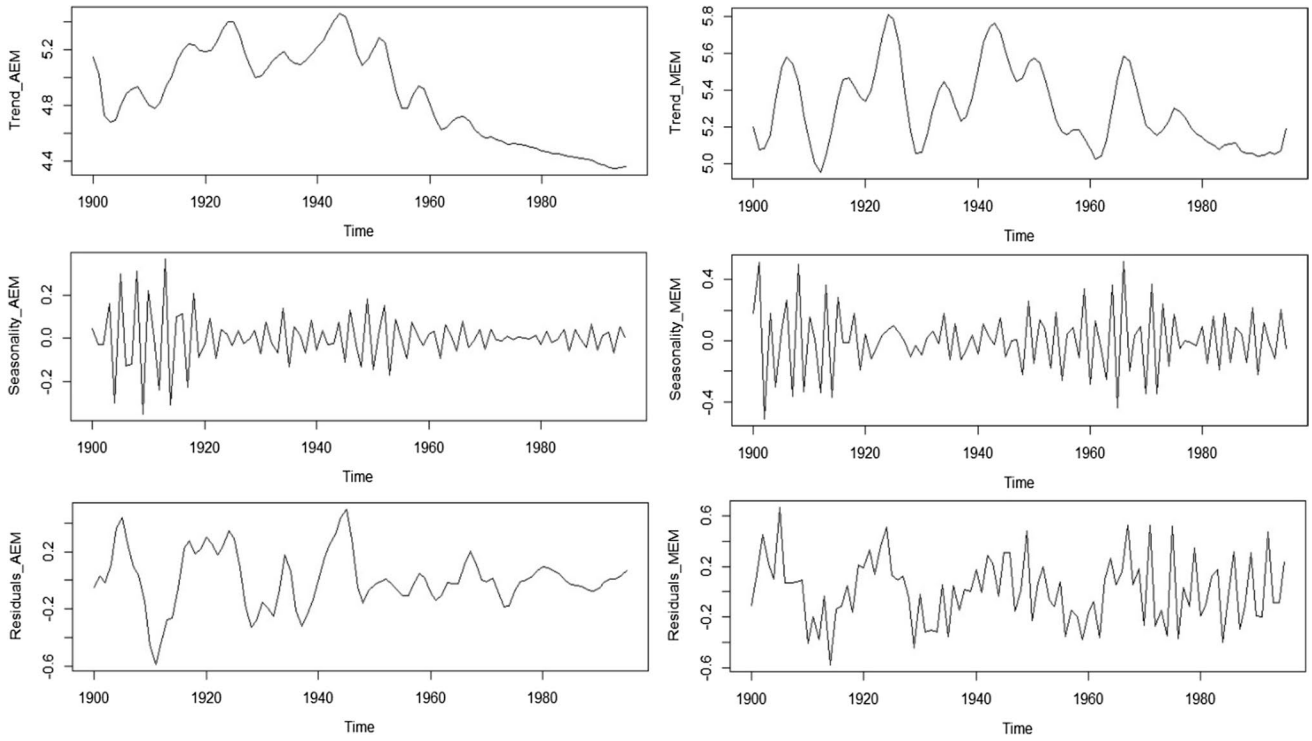

Fig. 6 The graphics of AEM and MEM series components

expected, it is indicated that the residual components are around 0.

The strong relationship between principal components is designated 4 and 10 due to the test, respectively. Thus, the SSA model parameters are selected at the end of this selection process as (W = 12, p = 4) and (W = 12, p = 10) for AEM and MEM variables. The RMSE values and the optimum models derived in ARIMA and SSA methods are calculated as in Table 3. The lowest RMSE values are obtained with the models created with the SSA for two variables.

The time series graphs of AEM and MEM predictions and 95% confidence interval values from 1996 to 2030 are represented in Fig. 8 for each model. Figure 8 indicates that the confidence limits obtained from ARIMA methods are estimated at extensive intervals. Although the SSA method predicts the upper and lower limits quite narrowly for the

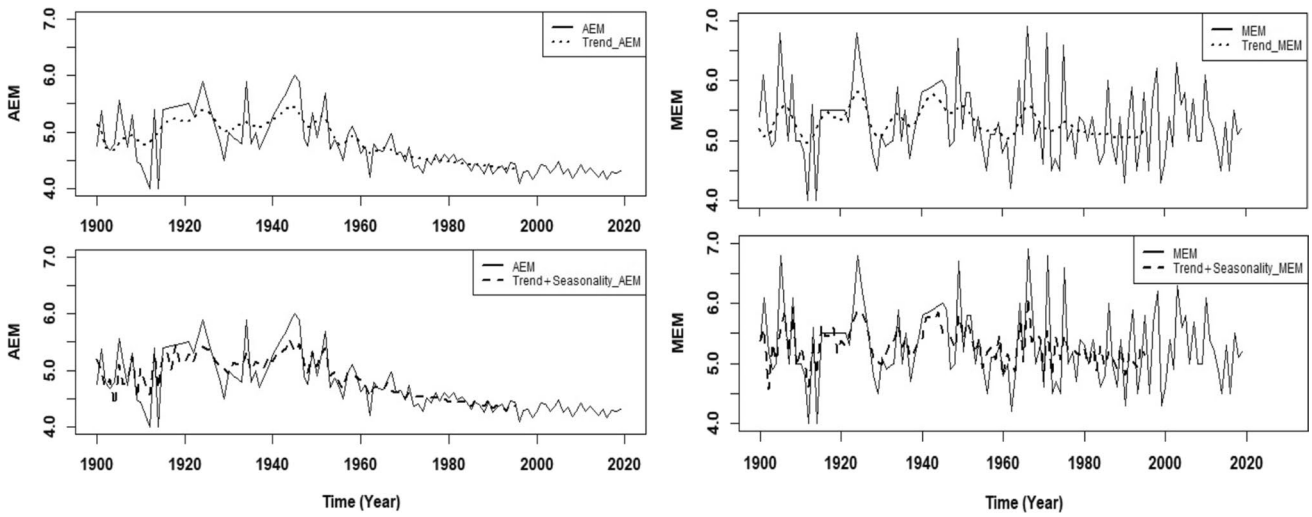

Fig. 7 The graphics of original series and the trend and trend + seasonal components

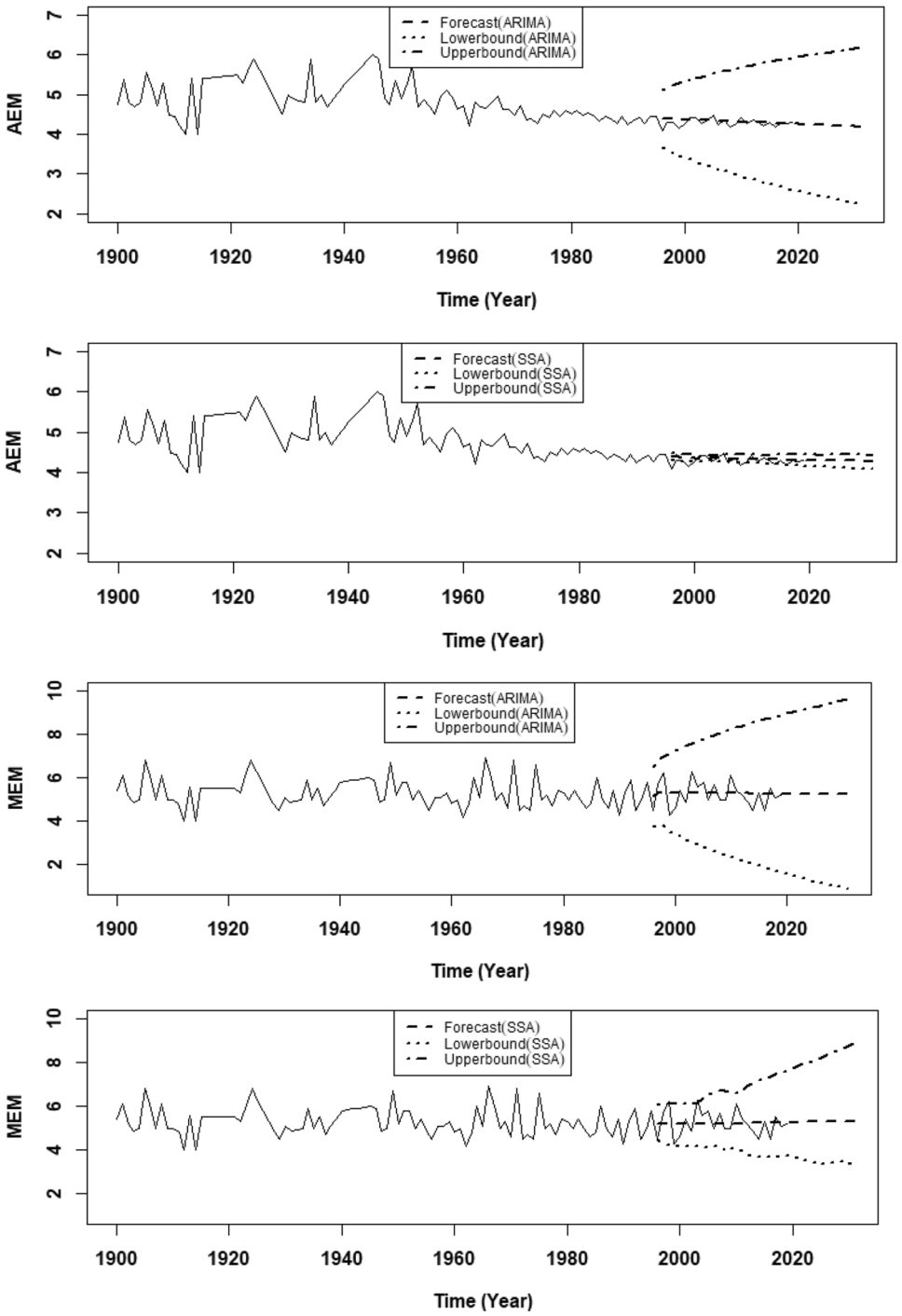

Fig. 8 The forecasts and confidence intervals of the AEM and MEM for each model

AEM estimation, it is seen that the same limits are calculated close to the real values in the MEM prediction.

According to the RMSE values given in Table 3, although the two methods have close ratios to each other, the best predictions are obtained by the SSA method. Thus, Table 4 shows the forecast values of the AEM and MEM from 2020 to 2030 according to the SSA method. In general, it is seen that the future predictions obtained in Table 4 are expected to continue with a decreasing slope due to the decreasing trend in actual values in recent years.

The results in Table 4 are also supported by Bayrak et al. (2015). They calculated that the probability of occurrence for the earthquakes with $M \geq 4.0$ is greater than 90%. Bulut et al. (2012) also found that micro and moderate sized earthquakes within up to 2030 can be occurred between the main fault and subsidiary faults in the EAF zone.

Table 4 Forecasted AEM and MEM (Mw) values with SSA models between years 2020 and 2030

Years	Variables	
	AEM	MEM
2020	4.259	5.260
2021	4.253	5.257
2022	4.248	5.254
2023	4.242	5.251
2024	4.236	5.248
2025	4.230	5.246
2026	4.225	5.243
2027	4.219	5.240
2028	4.213	5.237
2029	4.208	5.234
2030	4.202	5.231

Conclusion

Turkey and its surrounding area are known as an excellent natural laboratory to study tectonic escape-related deformation, and the consequent structures that include fold and thrust belts, suture zones, active strike-slip faulting, and active normal faulting and the associated basin formation. The EAFZ is one of the most important fault systems in and around Turkey.

The SSA technique was already known as a powerful tool in time series analysis. In this study, the SSA forecast skills were assessed and compared with the ARIMA model on an earthquake magnitude time series, known to have a more appropriate structure to forecast. This study illustrates that the SSA technique can be successfully used as a forecasting algorithm for earthquake size prediction. The SSA was able to model its structure and to forecast future earthquake magnitude than ARIMA model accurately. Moreover, the trend component obtained with SSA is a deterministic element for the assessment of earthquake magnitude.

The results also suggest that, even if there are essential components that may be extracted and forecasted using SSA, a significant fraction of the variability of those seismological time series does not seem to have an appropriate time structure to be forecasted.

References

Akkar S, Azak T, Çan T, Çeken U, Demircioğlu Tümsa MB, Duman TY, Erdik M, Ergintav, S, Kadirioğlu FT, Kalafat D, Kale Ö, Kartal RF, Kekovalı K, Kılıç, T, Özalp S, Altuncu Poyraz S, Şeşetyan K, Tekin S, Yakut A, Yılmaz MT, Yücemen MS, Zülfikar Ö (2018) Evolution of seismic hazard maps in Turkey. Bull Earthq Eng 16(8):3197–3228

Aksoy E, Inceoez M, Koçyiğit A (2007) Lake Hazar basin: A negative flower structure on the east anatolian fault system (EAFS), SE Turkey. Turk J Earth Sci 16(3):319–338

Allen M, Jackson J, Walker R (2004) Late Cenozoic reorganization of the Arabia-Eurasia collision and the comparison of short-term and long-term deformation rates. Tectonics, 23(2)

Arpat E, Şaroğlu F (1972) The East Anatolian fault system; thoughts on its development. Min Res Explor Inst Turkey Bull 78:33–39

Aslan E (1972) Magnitude and time distributions of earthquakes in Turkey. Bull Int Inst Seismol Earthq Eng 7:1–10

Başarır Baştürk N, Özel NM, Altınok Y, Duman TY (2017) Türkiye ve Yakın Çevresi için Geliştirilmiş Tarihsel Dönem (MÖ 2000-MS 1900-) Deprem Katalogu. Türkiye Sismotektonik Haritası Açıklama Kitabı, MTA Özel Yayınlar Serisi-35, 24

Bath M (1979) Seismic risk in Turkey-a preliminary approach. Tectonophysics 54:9–16

Bayrak E, Yılmaz Ş, Softa M, Türker T, Bayrak Y (2015) Earthquake hazard analysis for East Anatolian Fault Zone, Turkey. Nat Hazards 76(2):1063–1077

Bayrak Y, Öztürk S, Çınar H, Kalafat D, Tsapanos TM, Koravos GC, Leventakis GA (2009) Estimating earthquake hazard parameters from instrumental data for different regions in and around Turkey. Eng Geol 105 (3-4):200–210

Bayrak Y, Yılmazturk A, Ozturk S (2005) Relationships between fundamental seismic hazard parameters for the different source regions in Turkey. Nat Hazards 36:445–462

Broomhead DS, King GP (1986) Extracting qualitative dynamics from experimental data. Physica D 20(2–3):217–236

Bulut F (2017) Seismic and a-seismic tectonic motions along the East Anatolian Fault: Seismic Gap or Creep in the east of Hazar Lake? AKU. J Sci Eng 17:257–263

Bulut F, Bohnhoff M, Eken T, Janssen C, Kılıç T, Dresen G (2012) The East Anatolian Fault Zone: Seismotectonic setting and spatiotemporal characteristics of seismicity based on precise earthquake locations. J Geophys Res Solid Earth 117(B7)

Dargahi-Noubary GR (1986) A method for predicting future large earthquakes using extreme order statistics. Phys Earth Planet Inter 42:241–245

DEMA (2020) The Republic of Turkey Prime Ministry, Disaster & Emergency Management Authority, Presidential of Earthquake Department, https://deprem.afad.gov.tr/, (Access Date: 23 Dec 2020)

Deng C (2014) Time Series Decomposition Using Singular Spectrum Analysis, Master thesis, 81

Dewey JF, Hempton MR, Kidd WSF, Saroglu FAMC, Şengör AMC (1986) Shortening of continental lithosphere: the neotectonics of Eastern Anatolia—a young collision zone. Geological Society, London, Special Publications 19(1):1–36

Duman TY, Çan T, Emre Ö, Kadirioğlu FT, Başarır Baştürk N, Kılıç T, Arslan S, Özalp S, Kartal RF, Kalafat D, Karakaya F, Eroğlu Azak T, Özel NM, Ergintav S, Akkar S, Altınok Y, Tekin S, Cingöz A, Kurt Aİ (2018). 'Seismotectonics Database of Turkey'. Bull Earthq Engr 16:3277–3316. https://doi.org/10.1007/s10518-016-9965-9

Duman TY, Emre Ö (2013) The East Anatolian Fault: geometry, segmentation and jog characteristics. Geological Society, London, Special Publications 372(1):495-529

Emre Ö, Duman TY, Özalp S, Elmacı H, Olgun Ş, Şaroğlu F (2013) Açıklamalı Türkiye Diri Fay Haritası. Ölçek 1(1.250), 000, Maden Tetkik ve Arama Genel Müdürlüğü, Özel Yayın Serisi-30, Ankara-Türkiye (In Turkish)

Erdik M, Biro YA, Onur T, Sesetyan K, Birgoren G (1999) Assessment of earthquake hazard in Turkey and neighboring. Ann Geophys 42(6)

Fraedrich K (1986) Estimating the dimensions of weather and climate attractors. J Atmos Sci 43(5):419–432

Gao W, Guo J, Zhou M, Y H, Chen X, Ji B (2020) Gravity tides extracted from SSA-denoised superconducting gravity data with

the harmonic analysis: a case study at Wuhan station, China. Acta Geodaetica et Geophysica, 1–17
Ghil M, Vautard R (1991) Interdecadal oscillations and the warming trend in global temperature time series. Nature 350(6316):324–327
Golyandina N, Zhigljavsky A (2013) Singular Spectrum Analysis for time series. Springer Science & Business Media.
Guo J, Shi K, Liu X, Sun Y, Li W, Kong Q (2019) Singular spectrum analysis of ionospheric anomalies preceding great earthquakes: Case studies of Kaikoura and Fukushima earthquakes. J Geodyn 124:1–13
Hassani H, Yeganegi MR, Khan A, Silva ES (2020) The Effect of Data Transformation on Singular Spectrum Analysis for Forecasting. Signals 1:2
Helmstetter A, Sornette D (2003) Importance of direct and indirect triggered seismicity in the ETAS model of seismicity. Geophys Res Lett 30(11)
Hempton MR (1985) Structure and deformation history of the Bitlis suture near Lake Hazar, southeastern Turkey. GSA Bulletin 96(2):233–243. https://doi.org/10.1130/0016-7606(1985)96%3C233:SADHOT%3E2.0.CO;2
Hyndman RJ, Athanasopoulos G (2018) Forecasting: principles and practice. OTexts.
Jackson DD, Kagan YY (2006) The 2004 Parkfield earthquake, the 1985 prediction, and characteristic earthquakes: Lessons for the future. Bull Seismol Soc Am 96(4B):S397–S409
Kadirioğlu FT, Kartal RF, Kılıç T, Kalafat D, Duman TY, Azak TE, Emre Ö (2018) An improved earthquake catalogue (M≥ 4.0) for Turkey and its near vicinity (1900–2012). Bull Earthq Eng 16(8):3317–3338
Kagan YY (1993) Statistics of characteristic earthquakes. Bulletin of the Seismological Society of America 83(1):7–24
Kagan YY (2007) On Earthquake Predictability Measurement: Information Score and Error Diagram. Pure Appl Geophys 164:1947–1962
Kayabalı K, Akın M (2003) Seismic hazard map of Turkey using the deterministic approach. Eng Geol 69:127–137
Kumaresan R, Tufts DW (1980) Data-adaptive principal component signal processing. In 1980 19th IEEE Conference on Decision and Control including the Symposium on Adaptive Processes 949–954. IEEE.
Lai Y, Dzombak DA (2020) Use of the Autoregressive Integrated Moving Average (ARIMA) Model to Forecast Near-Term Regional Temperature and Precipitation. Weather Forecast 35(3):959–976
Moskvina V, Zhigljavsky A (2003) An algorithm based on singular spectrum analysis for change-point detection. Commun Stat - Simul Comput 32(2):319–352
Naim I, Mahara T (2018) Comparative Analysis of Univariate Forecasting Techniques for Industrial Natural Gas Consumption. Int J Image Graph Signal Process 10:33–44
Ogata Y (2017) Statistics of Earthquake Activity: Models and Methods for Earthquake Predictability Studies. Annu Rev Earth Planet Sci 45:497–527
Özel G (2011) A bivariate compound Poisson model for the occurrence of foreshock and aftershock sequences in Turkey. Environmetrics 22(7):847–856
Özel G Inal C (2008) The probability function of the compound Poisson process and an application to aftershock sequence in Turkey. Environmetrics: J Int Environmetrics Soc 19(1):79–85
Pereira de Albuquerque WC, Maciel CD (2001) Performance of ultrasound echo decomposition using singular spectrum analysis. Ultrasound Med Biol 27(9):1231–1238
Petersen MD, Cao T, Campbell KW, Frankel AD (2007). Time-independent and time-dependent seismic hazard assessment for the State of California: Uniform California Earthquake Rupture Forecast Model 1.0. Seismol Res Lett 78(1):99–109
Serita A, Hattor K, Yoshino C, Hayakawa M, Isezaki N (2005) Principal component analysis and singular spectrum analysis of ULF geomagnetic data associated with earthquakes
Shishegaran A, Taghavizade H, Bigdeli A, Shishegaran A (2019) Predicting the Earthquake Magnitude along Zagros Fault Using Time Series and Ensemble Model. Soft Comput Civ Eng 3(4):67–77
Silva ES, Hassani H, Heravi S (2018) Modeling European industrial production with multivariate singular spectrum analysis: A cross-industry analysis. J Forecast 37:371–384
Sivapragasam C, Liong SY, Pasha MFK (2001) Rainfall and runoff forecasting with SSA–SVM approach. J Hydroinf 3(3):141–152
Vautard R, Ghil M (1989) Singular spectrum analysis in nonlinear dynamics, with applications to paleoclimatic time series. Physica D-Nonlinear Phenomena 35:395–424
Westaway R (1994) Present-day kinematics of the Middle East and eastern Mediterranean. Journal of Geophysical Research: Solid Earth 99(B6):12071–12090
Xiao J, Zhu X, Huang C, Yang X, Wen F, Zhong M (2019) A new approach for stock price analysis and prediction based on SSA and SVM. Int J Inf Technol Decis Mak 18(01):287–310
Yarar R, Ergunay O, Erdik M, Gulkan P (1980) A Preliminary Probabilistic Assessment of the Seismic Hazard in Turkey. In: Proceedings of the 7th World Conference on Earthquake Engineering, Istanbul. 309–316
Yiou P, Baert E, Loutre MF (1996). Spectral analysis of climate data. Surv Geophys 17(6):619–663
Zhang Y, Yang H, Cui H, Chen Q (2020) Comparison of the ability of ARIMA, WNN and SVM models for drought forecasting in the Sanjiang Plain. China Natural Resources Research 29(2):1447–1464
Zhu F (2012) Modeling overdispersed or underdispersed count data with generalized Poisson integer-valued GARCH models. J Math Anal Appl 389(1):58–71